Chapter 2
The Atmospheric and Target Modulations of the Lasers

During the receiving and emitting of lasers in laser imaging, the interactions among atmosphere, targets, and the lasers, namely, the atmospheric and target modulations of the lasers, directly influence the waveform characteristics of the targeted laser echoes. As a result, various subsequent processes such as information and data acquisition, data processing, image generation, feature extraction, classification and recognition are directly or indirectly influenced. By taking the mechanism of the target detection based on a laser imaging system as the object, this chapter explores the atmospheric and target modulations of lasers. This chapter mainly studies the concepts and characteristics of the atmospheric and target modulations of lasers, the characteristics of the energy and signal modulations, and the influences of the atmospheric and target modulations.

2.1 The Concepts of the Atmospheric and Target Modulations of Lasers

The link of the target detection based on a laser imaging system is usually composed of a system platform, a laser source, the atmosphere, a laser imaging sensor, a GPS, an attitude measurement unit, a data acquisition and processing system, an image generation system, a feature extraction system, a classification and recognition system, a detection and location system, etc. The block diagram of the signal and data link for the target detection based on a laser imaging system constituted by the aforementioned parts is demonstrated in Fig. 2.1.

As demonstrated in the link shown in Fig. 2.1, the laser signals radiated by the laser source are expected to experience complicated interaction with the matters in the atmosphere while passing through the atmosphere. Meanwhile, the incident lasers on the target are expected to interact with the target, while the reflected lasers cannot reach the laser imaging sensor unless passing through the atmosphere.

Y. Hu, *Theory and Technology of Laser Imaging Based Target Detection*,
DOI 10.1007/978-981-10-3497-8_2

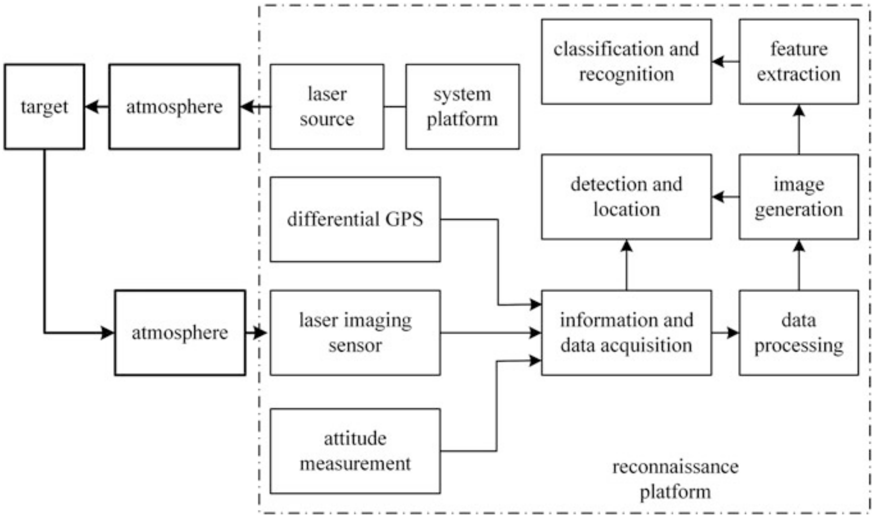

Fig. 2.1 The signal and data link for the target detection based on a laser imaging system

Therefore, while carrying out the target detection using laser imaging, laser signals require to contact and interact with the atmosphere and target respectively, so that they can be modulated.

The atmosphere is comprised of various gases and suspended impurity particles of various sizes, which show different components and chemical properties. When lasers propagate from the laser source to the targets, they are expected to interact with the gas molecules and particles in the atmosphere, which gives rise to the absorption, scattering, reflection, diffusion, refraction and diffraction phenomena. As to the main influences:

(i) the selective absorption of several gas molecules in the atmosphere for the lasers leads to the attenuation of the radiation intensity and the variation of the propagation direction of the lasers;
(ii) the scattering of the lasers by the suspended particles in the atmosphere results in the attenuated intensity and changed propagation direction of the lasers;
(iii) the violent change of the physical properties of the atmosphere leads to the flickers of the lasers and thus results in the modulation and variation of the lasers illuminance;
(iv) the variation of the physical properties of the atmospheric molecules and suspended particles results in the variation of the laser radiation;
(v) atmospheric turbulence gives rise to the random variation of the optical refractive index, resulting in the wave-front distortion, and thus changes the intensity and coherence of the lasers. All these indicate that the existence of the atmosphere changes the intensity, phase, polarization, and propagation

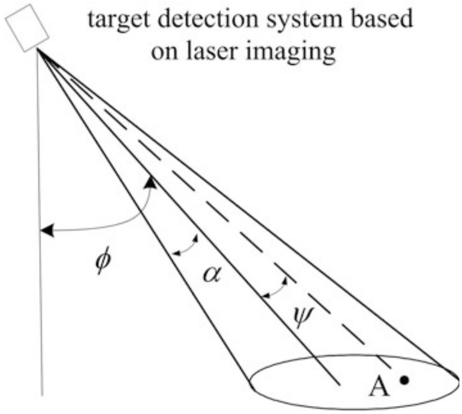

Fig. 2.2 The relationship between the laser spot and the target

direction of the laser signals, which is generally represented by the attenuation of the laser signals. Besides, the attenuation of the laser signals changes with the atmospheric conditions.

When it comes to the target modulation of lasers, the relationship between the laser echo signal reflected from any a point on the target and the target can be obtained according to that between the target and the incident beams shown in Fig. 2.2 [1]:

$$f_i(t) = a_i \exp[-k(t_i - t)^2/\tau^2] \cdot g(\psi) \cdot \cos(\zeta) \cdot h/s_i^2 \tag{2.1}$$

where, a_i represents the surface reflectivity, characterizing the attribute of the targets, while t_i indicates the echo time-delay of the corresponding target sampling point, representing the spatial distribution of the targets. τ denotes the width of the laser pulses and $g(\psi)$ is the energy distribution function of the laser spots, which is considered to be complied with the Gaussian distribution. ζ signifies the angle between the incident angle of the lasers and the normal line on the surface of the targets. h is a coefficient related to the response of the detector, effective receiving area and atmospheric attenuation. s_i represents the distance between the target sampling point and the target detection system based on laser imaging.

As shown in Fig. 2.2, ϕ indicates the angle between the central axis of the laser beams and the nadir, while α represents the half divergence angle of the lasers. ψ signifies the angle between any a beam in the lasers and the central axis.

The echo signal of the laser reflected by the target is the composition of the echo signals from various points on the target, and can be expressed as:

$$p(t) = \int_{\psi 1}^{\psi 2} f_i(t) d\psi \tag{2.2}$$

It can be seen from formulas (2.1) and (2.2) that echo signals of the laser are modulated by the various sampling points on the target form both the time and the space. The waveform characteristic of the target echo is a combined modulation function related to the time (echo time-delay), space (the position in light spots) and attributes (back-reflection and structural fluctuation) of the various parts in the targets [2]. Meanwhile, different target types lead to the generation of the target echoes with different waveform characteristics such as width, amplitude, phase and so on.

When it comes to the lexical meaning, modulation refers to changing several parameters (such as amplitude, frequency, etc.) of a signal (such as light, electrical oscillation and so on) according to the variation of the other signal (modulation, acoustic and TV signals). The interactions of the atmosphere, target and the lasers lead to the direction, energy, shape, amplitude and width of the reflected laser signals different from those of the incident pulsed lasers, which coincides with the implicit meaning of the modulation. Therefore, it is considered that the target echo is generated by the atmospheric and target modulations of the pulsed lasers, namely, the product of the atmospheric and target modulations of the lasers. Hence, the atmospheric and target modulations of the lasers refer to the phenomenon that the interactions of the lasers with the atmosphere and the target lead to the variation of the parameters of the laser signals. Meanwhile, the parameters of the laser signals are changed with the atmospheric components and the characteristics of the target.

The atmospheric modulation of the lasers is represented by the absorption, scattering and turbulence phenomena, all of which attenuate the signal intensity. In contrast, the target modulation of the lasers is slightly complicated and represented by the reflection and scattering phenomena. However, target modulation gives rise to the variations of several or all of the parameters including the intensity of the echo signals, and the width, shape and number of the pulses. Besides, the variations of these parameters are inevitably related to the characteristics of the target, which provides conditions for obtaining the characteristics of the targets based on the echo signals of the laser.

2.2 The Atmospheric Modulation of the Lasers

2.2.1 The Absorption Characteristics of the Atmosphere for the Lasers

The atmospheric absorption of the lasers refers to the fact that the gases such as H_2O, CO_2, O_3, N_2O, CO and CH_4 in atmosphere experience energy state transition under the influence of the lasers. In this way, light energy is converted into other forms such as power and heat energy or distributed in other types of spectra, which thus results in the energy attenuation of the light beams. The energy attenuation caused by the absorption of lasers by the atmosphere can be described by the

Lambert-Bougner law. Assume that the intensity of the laser (with the intensity being $I(v)$) is $I(v) + dI(v)$ after passing through the atmosphere layer that is dh thick, we obtain:

$$dI(v) = -I(v)\beta_{ab}(v, h)dh \tag{2.3}$$

where, $\beta_{ab}(v, h)$ is called the absorption coefficient. By solving formula (2.3), we obtain the following formula:

$$I(v) = I_0(v)\exp[-\int_{h_0}^{h_1} \beta_{ab}(v, h)dh] \tag{2.4}$$

If the atmosphere between h_0 and h_1 is homogeneous, and $\beta_{ab}(v, h)$ is unrelated with the thickness h of the atmosphere layer, formula (2.4) can be simplified as:

$$I(v) = I_0(v)\exp[-\beta_{ab}(v)L] \tag{2.5}$$

where, L represents the distance between h_0 and h_1.

By transforming formula (2.5), the parameter τ that can quantitatively describe the attenuation degree caused by the atmospheric absorption is obtained:

$$\tau = \frac{I(v)}{I_0(v)} = \exp[-\beta_{ab}(v)L] \tag{2.6}$$

where, the parameter τ is called the transmittance, namely, the ratio of the intensity of the laser after propagating for the distance of L to that of the output laser. The dimension of the absorption coefficient β_{ab} is L^{-1} with the commonly used unit being km^{-1}. For the convenience of calculation, the two sides of formula (2.6) are taken the logarithm and then enlarged for 10 times. Meanwhile, decibel dB is utilized to represent I/I_0, and the unit of β_{ab} is changed as $dB\ \text{km}^{-1}$.

The absorption of light energy by these gases makes the absorption spectrum of the atmosphere become several separated absorption bands, which are composed of considerable amounts of the spectral lines with different overlapping degrees and intensities. The overlapping degree of these spectral lines is related to the half width of the position of the spectra lines and the type of the absorption molecules (Fig. 2.3). Table 2.1 illustrates the wavelengths of the absorption line and band of the gas molecules.

Theoretically speaking, the absorption coefficient can basically be obtained by determining the intensity and position of the absorption line or band of the molecules. Then, the attenuation of the light intensity induced by the atmospheric absorption can be calculated according to the Lambert-Bougner law. However, as a matter of fact, absorption coefficient is not only related to the type of the gas

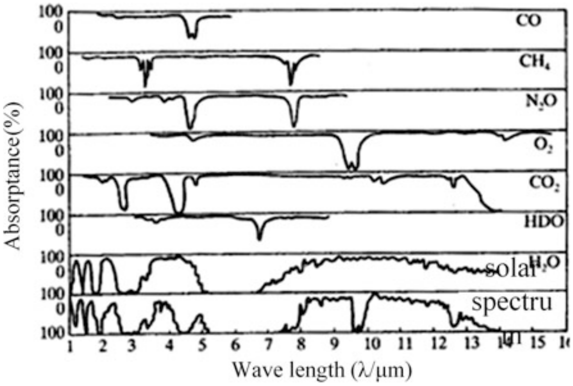

Fig. 2.3 The absorption spectra of the various absorption components in the atmosphere

Table 2.1 The absorption lines of the main gas molecules absorbing the light energy (μm)

Molecule	Type	Ultraviolet region	Visible region	Infrared region	
				Strong absorption line	Weak absorption line
CO	Linear	–	–	4.67	1.19, 1.57, 2.34
CH_4	Symmetric gyroscope	–	–	3.31, 3.8, 7.6	6.5
N_2O	Linear	–	–	4.5	3.9, 4.05, 7.7, 8.6, 17.1
O_2	Linear	0.175–0.2026 0.242–0.26	0.63, 0.69, 0.76		1.0674, 1.2683, 3.23, 10.33
CO_2	Linear	–	–	2.7, 4.3, 14.7	0.4–1.24, 1.4, 1.6, 2.0, 4.8, 5.2, 9.4, 10.4, 11.4–20
H_2O	Asymmetric gyroscope	–	0.72	1.87, 2.70, 2.67	–
HDO	–	–	–	3.7	–

molecules, but also the following factors: (i) absorption coefficient is changed with the wavelength; (ii) temperature and pressure can influence the shape of the absorption lines, and then affects the absorption coefficient; (iii) absorption coefficient is a function of the concentration of the absorption molecules; and (iv) the concentration, temperature and total pressure of the absorption molecules change with the geographical position, altitude, season and weather. The existence of the aforementioned factors makes it difficult to determine the absorption coefficient. In order to satisfy the requirements of the engineering practice, the following methods including the absorption coefficient method (line-by-line method), band model, LOWTRAN based semi-empirical method are primarily adopted to determine the atmospheric transmittance [3].

2.2.2 The Characteristics of Atmospheric Scattering for the Lasers

When lasers propagate in the atmosphere, apart from the energy attenuation caused by the selective absorption of the atmospheric molecules, there also exists the energy attenuation induced by atmospheric scattering. The so called atmospheric scattering refers to the fact that the atmospheric molecules and aerosol particles are polarized under the irradiation of the lasers, and thus produce the vibrating electromagnetic multipoles. Afterwards, electromagnetic vibration is generated by the vibrating multipoles, and irradiates secondary electromagnetic waves to various directions to form the light scattering. The energy distribution of the scattered light is related to the wavelength and intensity of the incident light, and the size and shape of the particles, as well as the refractive index. Pure scattering not consumes the total energy of the laser beams, but is expected to change the original spatial distribution of the energy of the laser beams. Therefore, the scattering process will attenuate the energy of the laser beams in the original propagation direction.

After the one-wavelength laser with the wavelength and power being λ and $P_\lambda(0)$ respectively propagates in the inhomogeneous media for x, the power of the laser beams is attenuated as $P_\lambda(x)$ after the scattering process. Then, the relationship between the distance x and the power $P_\lambda(x)$ is expressed as follows:

$$P_\lambda(x) = P_\lambda(0)\exp[-\gamma(\lambda)x] \tag{2.7}$$

where, $\gamma(\lambda)$ represents the scattering coefficient and is the function of the wavelength λ of the incident light.

A parameter $\tau_S(x,\lambda)$ that can characterize the attenuation capacity of the atmospheric scattering is obtained by transforming formula (2.7). This parameter is the function of the wavelength λ and distance x, and is defined as the atmospheric transmittance:

$$\tau_S(x,\lambda) = \frac{P_\lambda(x)}{P_\lambda(0)} = \exp[-\gamma(\lambda)x] \tag{2.8}$$

In general, the atmospheric scattering of the lasers is composed of two parts, namely, the scattering of the atmospheric molecules and suspended particles (aerosols in general) in the atmosphere. Therefore, scattering coefficient can be divided into two coefficients, namely:

$$\gamma(\lambda) = \gamma_m(\lambda) + \gamma_a(\lambda) \tag{2.9}$$

where, $\gamma_m(\lambda)$ and $\gamma_a(\lambda)$ represent the scattering coefficients of the atmospheric molecules and aerosols respectively.

Table 2.2 The size and concentration of the various particles in the atmosphere

Particle type	Radius (μm)	Concentration (cm^{-3})
Air molecules	10^{-4}	10^{19}
Aitken nucleus	10^{-3}–10^{-2}	10^{2}–10^{4}
Haze particles	10^{-2}–100	10^{1}–10^{3}
Fog droplet	10^{0}–10^{1}	10^{1}–10^{2}
Cloud droplet	10^{0}–10^{2}	10^{1}–10^{2}
Raindrop	10^{2}–10^{3}	10^{-5}–10^{-3}
Ice crystals and snowflakes	10^{3}–10^{4}	–
Dust	10^{2}–10^{3}	10^{0}–10^{1}

It can be seen from formula (2.9) that if the scattering coefficient $\gamma(\lambda)$ is known, the atmospheric transmittance $\tau_S(x, \lambda)$ of the laser after propagating for the distance of x can be obtained according to formula (2.8).

The sizes of the particles in atmosphere vary greatly, as shown in Table 2.2. The particles with different sizes are endowed with different scattering properties. The scattering properties of the particles are basically determined by the ratio of the particle size to the incident wavelength. To be specific, different particle sizes indicate different ratios of the particle size to the incident wavelength, which call for different theoretical models. When the particle size is much smaller than the wavelength, the simple Rayleigh scattering model is applicable here. In case the particle size is nearly equal to the wavelength, it is appropriate to adopt the complicated Mie scattering model. When the particle size is much greater than the wavelength, the scattering is considered to be non-selective.

1. **Rayleigh scattering**

Rayleigh scattering occurs when the wavelength of the lasers is much greater than the radius of the particles, and mainly takes place in gas molecules. Therefore, Rayleigh scattering is also called the molecular scattering. The scattering cross section of the lasers is utilized to describe the scattering ability of the target to the incident lasers. Similarly, the scattering cross section σ_m can be used to represent the scattering ability of the gas molecules. According to this parameter, it is defined that the energy of the incident lasers that pass through this cross section σ_m is equal to the total power scattered in various directions of this molecule, namely:

$$\sigma_m E_0 = I \tag{2.10}$$

where, E_0 represents the irradiance of the incident lasers on the cross section, and I indicates the scattering intensity of the molecules.

Another expression of the scattering cross section can be obtained by transforming formula (2.10), namely:

$$\sigma_m = \frac{E_0}{I} \tag{2.11}$$

That is to say, the scattering cross section σ_m is the ratio of the scattering intensity to the irradiance of the incident lasers of the molecule. It is worth noting is that the scattering cross section is different from the geometrical cross section in terms of the meaning and value.

According to the Rayleigh molecular scattering formula, the total scattering cross section of a single molecule is demonstrated as [4]:

$$\sigma_m = \frac{8\pi^3(n^2-1)^2}{3N^2\lambda^4} \tag{2.12}$$

where, n represents the refractive index of air, and N indicates the number of the molecules per unit volume. λ signifies the wavelength of the incident light.

It can be seen from formula (2.12) that the scattering cross section of the molecules is inversely proportional to the fourth power of the wavelength. Therefore, it is obtained that molecular scattering has a particularly significant influence on the light wavebands with small wavelength in Rayleigh scattering. For example, if $\lambda = 0.55$ μm, then $\sigma_m \approx 4.6 \times 10^{-27}$ cm^2; while when $\lambda = 5.5$ μm, we obtain $\sigma_m \approx 4.6 \times 10^{-31}$ cm^2 under the standard state.

When the scattering process happens on the small solid particles, if the radius of the particles satisfies the condition of $2\pi\lambda/r \leq 1$, it is still appropriate to adopt the Rayleigh scattering model. Accordingly, the scattering cross section is changed as:

$$\sigma_p = \frac{128\pi^3 r^6}{3\lambda^4}\left(\frac{n^2-1}{n^2+2}\right)^2 \tag{2.13}$$

where, n and r represent the refractive index and the radius of the particles separately.

According to formula (2.13), the scattering cross section of the condensation nucleus with the wavelength, radius and refractive index being 1 μm, 0.032 μm and 1.60 respectively is 1.17×10^{-14} cm^2. It can be seen from the calculation result of the scattering cross section of single a molecule or particle that this value is very small. However, if the scattering cross sections of all the atmospheric molecules or particles per unit volume are added together, the obtained scattering cross section will be great in value. The volume scattering coefficient β_m is the ratio of the total energy scattered in various directions of the gas molecules per unit volume to the irradiance of the incident light. It represents the sum of the scattering cross sections of each molecule per unit volume, namely $\beta_m = N\sigma_m$:

$$\beta_m = N\sigma_m = \frac{8\pi^3(n^2-1)^2}{3N\lambda^4} \tag{2.14}$$

where, N indicates the number of the gas molecules per unit volume, with the dimension being L^{-3}. Therefore, the dimension of β_m is L^{-1}. If there are N particles of same size per unit volume, similarly, the volume scattering coefficient β_p of the particles can be obtained:

$$\beta_p = N\sigma_p = \frac{128\pi^3 r^6 N}{3\lambda^4}\left(\frac{n^2-1}{n^2+2}\right)^2 \tag{2.15}$$

Unlike gas molecules, particles generally are not consistent. As a result, it is difficult to calculate the volume scattering coefficient of the particles using the linear superposition. Instead, the distribution function requires to be utilized to solve the integration.

2. **Mie scattering and Non-selective scattering**

Mie scattering occurs when the particle size is nearly equal to the wavelength of the laser beams, and primarily happens on the fallout and aerosol particles. The refractive indexes of these particles are significantly different from that of the gas molecules. Compared with the Rayleigh scattering, Mie scattering is endowed with the following characteristics:

(i) The distribution of the intensity of the scattered light becomes increasingly complicated with the angle: the greater the particles compared with the wavelength, the more complicated the distribution is;
(ii) With the increase of the particle size, the ratio of the forward scattering to the backscattering is increased, leading to the increased lobe of the forward scattering;
(iii) When the ratio of the particle diameter to the wavelength increases, the scatting process presents increasingly insignificant dependence on the wavelength.

The particles where Mie scattering occur are composed of considerable amounts of closely arranged molecules, which form a multipole subarray. The vibrating multipoles are expected to be produced by the multipole subarray under the motivation of the incident lasers, and then irradiate outwardly the secondary electromagnetic waves, namely, the partial waves. Later, the partial waves are overlapped in the far field to form the scattered waves.

The scattering interface σ_p of the particles with Mie scattering is endowed with the same definition with that of the particles with Rayleigh scattering. That is to say, the power of the incident waves on σ_p is equal to the total power scattered in various directions of this particle. The Mie scattering cross section of single a particle can be obtained using the distribution function of the intensity of the Mie scattering [5]:

$$\sigma_p = \frac{\lambda^2}{2\pi} \sum_{n=1}^{\infty} (2n+1)(|a_n|^2 + |b_n|^2) \tag{2.16}$$

The scattered waves generated in the Mie scattering are composed of multiple partial waves. Therefore, a_n and b_n in formula (2.16) represent the complex amplitudes of the electric wave and magnetic wave of the nth partial wave separately.

The scattering efficiency factor Q_{sc} can be obtained by dividing the two sides of formula (2.16) using the geometric cross section πr^2, namely:

$$Q_{sc} = \frac{2}{v^2} \sum_{n=1}^{\infty} (2n+1)(|a_n|^2 + |b_n|^2) \tag{2.17}$$

where, v is called the scale parameter, and $v = 2\pi r/\lambda$. The scattering efficiency factor Q_{sc} reflects the ability of the geometric cross section per unit in scattering light-wave. Figure 2.4 illustrates the curve describing the variation of the scattering efficiency factor Q_{sc} of the spherical water drops with the scale parameter when the refractive index is $n = 1.33$. It can be discovered from the figure that when the value of the scale parameter is small, the value of the scattering efficiency factor Q_{sc} is far smaller than 1. That is to say, the scattered energy is far smaller than the incident energy of the particles. With the increase of the scale parameter v, the value of the scattering efficiency factor increases rapidly with the maximum value being close to 4, accompanying with the appearance of the damped oscillation. Finally, the value is converged to 2.

Since the scattering process is incoherent, the luminous flux of the volume scattering is equal to the sum of the luminous fluxes of each particle in the scatterer. According to the definition of the scattering interface, volume scattering interface is equal to the sum of the scattering cross sections of each particle. Assume that there are N particles per unit volume, the volume scattering coefficient is expressed as:

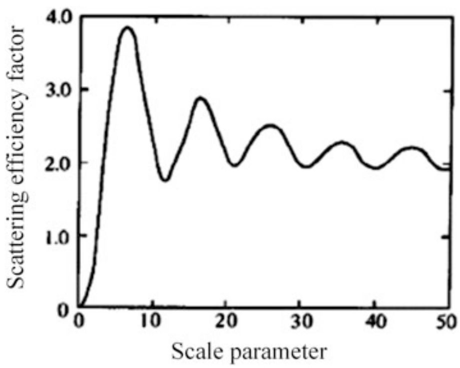

Fig. 2.4 The variation curve of the scattering efficiency factor of the spherical water drops with the scale parameter [6]

$$\beta_p = N\sigma_p = \frac{N\lambda^2}{2\pi}\sum_{n=1}^{\infty}(2n+1)(|a_n|^2 + |b_n|^2) \tag{2.18}$$

When the particle size is far greater than the wavelength of the lasers, non-selective scattering is expected to take place. Under such circumstance, the scattering intensity has nothing to do with the wavelength, and lasers with different wavelengths show the same scattering intensity.

3. **Multiple scattering**

The Rayleigh scattering, Mie scattering, and non-selective scattering are all analyzed based on the following conditions: the scattering process of each particle is independent of other particles, and particles merely scatter the direct light rays such as the incident light of the laser source or the lasers reflected by the target. This is the so called single scattering. As a matter of fact, a scatterer usually contains multiple scattering particles. As a result, apart from the direct lights, each scattering particle is likely to be exposed to the scattered lights of other particles, and therefore scatters these lights. Therefore, before being emitted from the scatterer, several lights that have been scattered once are likely to be scattered once again or for multiple times, which is the so called multiple scattering. Although multiple scattering has a little influence on the total light energy eliminated from the direct lights, it greatly changes the patterns of the compound distribution of the scattering intensities for all particles [5].

2.2.3 The Atmospheric Turbulence of Lasers

Atmospheric turbulence is an irregular motion of each atmospheric molecule group and is different from the mean motion of the overall atmosphere. The micro and random variation of the atmospheric temperature caused by human activities and solar irradiation is expected to randomly change the wind speed of the atmosphere, and thus forms the atmospheric turbulence. Meanwhile, the random variation of the atmospheric temperature is supposed to lead to the random variation of the atmospheric density and then that of the atmospheric refractive index. Furthermore, the cumulative effect of the random variation of the refractive index gives rise to the obvious inhomogeneity of the profile of the atmospheric refractive index. As a result, the wave-front of the light beams turbulently propagating in the atmosphere randomly fluctuates. In this way, a series of atmospheric turbulence effects including intensity scintillation, beam extension, phase fluctuation, jitter of source images and beam drift generated during the propagation processes of the lasers are triggered.

The degree and form of the influence of the atmospheric turbulence on the beam characteristics are related to the relative sizes of the diameter d of the beams and the turbulent scale l [6]. In case $d \gg 1$, that is, the diameter of the laser beams is far greater than the turbulent scale, the section of the laser beams is expected to contain numerous vortexes, each of which diffracts the small part of the light beams irradiated on them. As a result, the intensity and phase of the light beams present random variation in terms of the time and space. Meanwhile, the area of the light beams expands increasingly, which results in the generation of the effects such as intensity scintillation, beam extension and phase fluctuation. When $d \cong l$, turbulence gives rise to the random deflection of the section of the light beams, leading to the fluctuated angle of arrival. As a result, the source image is supposed to dither on the sensitive surface of the detector. While, as $d \ll 1$, that is, the diameter of the laser beams is far smaller than the turbulent scale, light beams are randomly deviated under the influence of the turbulence, causing the generation of the beam drift. What is worth noting is that turbulence induced effects are mutually related, and the turbulent scale is within certain a range. The vortexes of different sizes play their own roles respectively.

1. **Intensity scintillation**

Intensity scintillation is the most common and obvious effect caused by the atmospheric turbulence. Intensity scintillation refers to the phenomenon that lasers experience intensity fluctuation while propagating in the atmosphere. It is a kind of power modulation of the received signals induced by the atmospheric turbulence. The fundamental reason leading to the intensity scintillation is the inhomogeneous optical properties in certain an area of the atmosphere nearby the ground. When laser beams propagate the areas with varying temperature, the density and refractive index of the air are changed, which makes the laser beams deviate from the original propagation direction. As a result, the section of the light beams is varied, accompanying with the variation of the angular distribution of the laser energy within the section of the light beams. Since the inhomogeneity of the optical properties of the atmosphere is unstable and varies randomly, the influence of the intensity scintillation is therefore unstable and random. The main influence of the intensity scintillation on the receiving part of the target detection system based on laser imaging is the scintillation modulation. That is to say, intensity scintillation leads to the random variation of the energy of the received lasers reflected by the targets in a certain form, and the frequency generally varies in the range of 2.5–450 Hz.

Since there exists scintillation in the intensity of the received lasers reflected by the targets, it is necessary to measure this scintillation using a parameter. Therefore, the variance $\sigma^2_{\ln I}$ of the intensity logarithm $\ln I$ is commonly utilized to quantitatively describe the scintillation degree of the intensity. Both the measured data and theoretical studies demonstrate that in weak fluctuation regions, the variance of the intensity logarithm satisfies the following condition [4]:

$$\sigma^2_{\ln I} = C_o C_n^2 k_o^{7/6} z^{11/6} \tag{2.19}$$

where, C_o is a constant, and is taken as 0.496 and 1.23 respectively for the spherical and plane waves. C_n represents the structure constant of the atmospheric refractive index ($m^{-2/3}$), while k_o indicates the wavenumber and $k_o = 2\pi/\lambda$. z signifies the propagation distance of lasers (m).

It can be seen from formula (2.19) that the variance $\sigma^2_{\ln I}$ of the intensity fluctuation is in direct proportion to the structure parameter C_n^2 of the atmospheric refractive index and $k_o^{7/6}$. C_n^2 reflects the degree of the turbulence, which indicates that the intensity fluctuation is directly proportional to the turbulence intensity. The stronger the turbulence is, the more obvious the fluctuation of the light intensity in the receiving part. k_o is inversely proportional to the wavelength: the shorter the wavelength, the more obvious the intensity fluctuation. Besides, the variance of the intensity fluctuation is in direct proportion to the 11/6 power of the propagation distance z, which demonstrates that the farther the propagation distance, the more obvious the intensity fluctuation is.

While as the light beams undergo the slope-way transmission from the ground to the air or from the air to the ground, the aforementioned calculation formula of the variance of the intensity logarithm can be rewritten as [4]:

$$\sigma^2_{\ln I} = C_o k_o^{7/6} \int_{h_o}^{h_T} C_n^2(h)(\sec \acute{\omega})^{11/6} h^{5/6} dh \tag{2.20}$$

where, $\acute{\omega}$ represents the zenith angle in the transmission path of the light beams, while h_o indicates the launching height of the light source, and refers to the target height. h_T denotes the height of the receiving part in the system.

In the transmission from the surface to the air with $\psi < 60°$, the typical value of $\sigma^2_{\ln I}$ is 20%, which can be reduced to 4% in the case of favorable visibility. The upper limit of $\sigma^2_{\ln I}$ can be estimated using the following formula:

$$\sigma^2_{\ln I} < 0.436 \left(\frac{\lambda}{2.1 \rho_0 \vartheta_0} \right)^{5/6} \tag{2.21}$$

where, $\vartheta_0 = 0.508 \lambda^{6/5} (\cos \acute{\omega})^{8/5} \left[\int_{h_o}^{h_T} C_n^2(h) h^{5/3} dh \right]^{-3/5}$ represents the isoplanatic angle, with the typical value being 10 μrad in the visible light bands and usually varying from 3 to 10 μrad. $\rho_0 \sim \left(C_n^2 k_o^2 R \right)^{-3/5}$ indicates the coherent length of the turbulence, and is related not only to the turbulence intensity, but also to the wavelength and propagation distance. Its typical value is 10 cm in the visible light bands, and usually in the range of 5–20 cm.

According to the test on the theoretical formula (2.20), when $\sigma^2_{\ln I}$ is small, it is in direct proportion to C_n^2. However, as C_n^2 increases to some extent, $\sigma^2_{\ln I}$ basically maintains certain a fixed value and even reduces sometimes, which is called the saturated scintillation. Due to the existence of the saturated scintillation, the result of formula (2.20) is not coincident with the observed intensity fluctuation. Therefore, another expression is required to be utilized to describe the intensity fluctuation. The intensity variance $\sigma_I^2 = (\overline{I^2} - \bar{I}^2)/\overline{I^2}$ of the plane waves is expressed as [6]:

$$\sigma_I^2 = \begin{cases} 1 + \frac{2.03}{\left(\sigma_o^2\right)^{1/6}} & \sigma_o^2 = \left(\frac{2\pi}{l_o}\right)^{7/3} \quad C_n^2 z^3 \to \infty \\ 1 + \frac{0.86}{\left(\sigma_0^2\right)^{2/5}} & \varsigma = \frac{\lambda z}{l_0^2} \to \infty \end{cases} \tag{2.22}$$

The intensity variance $\sigma_I^2 = (\overline{I^2} - \bar{I}^2)/\overline{I^2}$ of the spherical waves is demonstrated as [6]:

$$\sigma_I^2 = 1 + \frac{0.86}{\left(\sigma_0^2\right)^{2/5}} \tag{2.23}$$

2. **Beam expansions**

Beam expansions refer to the fact that the spot area on the receiving system is larger than that generated after lasers propagating in the free space. The effective diameter of the expanded light spots is expressed as:

$$d_c = d_o \left(\frac{I_o}{\bar{I}_r}\right)^{1/2} \tag{2.24}$$

where, d_o represents the diffraction limited diameter of the light spots, and I_o indicates the limited intensity of the emitted light beams. $\bar{I}_r$ denotes the received average intensity.

The root mean square is utilized to represent the size of the beam extension. Then, the root mean square of the expanded light beams induced by the atmospheric turbulence is expressed as [7]:

$$\sigma_\theta = 1.71 C_n^2 R^{1/2} D^{1/6} \tag{2.25}$$

where, C_n represents the structure constant of the atmospheric refractive index, and R indicates the distance between the target and the receiving part of the target detection system based on laser imaging. D denotes the transmitting aperture of lasers.

Figure 2.5 illustrates the values of the beam extension under different intensities of atmospheric turbulence when the transmitting aperture is 10 cm. As observed in the figure, the extension of the laser beams caused by the turbulence is generally small when the imaging distance is small. In such case, the influence on the echoes can be ignored. However, in the case of long-distance imaging, the extension of the

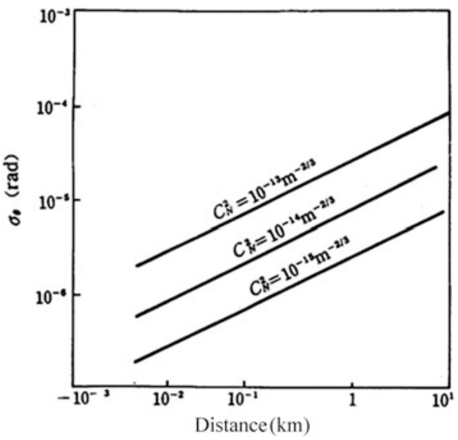

Fig. 2.5 The broadening of the beam angle of the root mean square induced by the atmospheric turbulence

laser beams induced by the turbulence is great. Under such circumstance, the influence on the echoes cannot be ignored.

3. **Phase fluctuation**

The fluctuation and inhomogeneity of the atmospheric refractive index caused by the atmospheric turbulence is expected to distort the wave-front in the transmission of the laser beams. With the increases of the propagation distance and time, the phase of the laser beams that reach the receiving optical aperture of the laser imaging system is expected to present significant irregular variation, which is called the phase fluctuation.

The intensity scintillation in the propagation direction is the function of the 3D space and time. Therefore, the inhomogeneity and random fluctuation of the refractive index within the section of the light beams are supposed to lead to the unequal fluctuations of each optical path, and thus produces the phase jitter. In the coherent laser imaging system, the coherence can be obviously destroyed by the phase jitter under the influence of the atmospheric turbulence. Consequently, beams are diverged with the shift of the frequency, leading to the blurred laser images.

4. **Source images Jitter**

When the diameter d of the light beams is close to the turbulent scale l, the influence of the atmospheric turbulence is primarily demonstrated as follows: the fluctuated atmospheric refractive indexes in different parts within the interface of the light beams result in the different phase shifts of the different parts in the wave-front of the light beams. In this way, the randomly fluctuated equiphase surfaces are generated. Later, such phase distortion leads to the fluctuation of the wave-front angle of the light beams, resulting in the jitter of the light spots in the receiving part, which gives rise to the jitter of the image points in the laser source, namely, source images jitter. During the dithering of the source images, the propagation direction of the laser beams randomly changes with the statistical average direction as the center.

The dithering degree of the source images is represented by the deflection angle between the actual direction of the laser beams and the statistical average direction, and the variation range of this angle is demonstrated as [7]:

$$(\Delta\theta)^2 = 1.048(A_C)^{-\frac{1}{3}}RC_n^2 \tag{2.26}$$

where, A_C represents the area of the receiving aperture of the target detection system based on laser imaging, and R indicates the distance between the target and the target detection system.

The jitter of the image points is unrelated to the wavelength, and the dithering frequency varies from several to dozens of Hertz. The dithering angle is associated with the geographic position and weather, with the maximum value being less than or equal to 50 μrad.

5. **Beam drift**

Beam drift refers to the random movement of the central position of the light spots under the disturbance of the atmospheric turbulence. After light beams propagate in the air for a period of time, the inhomogeneity of the refractive index of the atmospheric vortexes larger than that of the light beams is likely to result in the random deviation of the propagation direction of the light beams. Meanwhile, the central position of the light beams in the plane that is perpendicular to the propagation direction is supposed to vary randomly.

The drift effect of the light beams can be represented by the statistical variance $\langle \rho_c^2 \rangle$ of the displacement of the light beams. Under the approximation in geometrical optics, the statistical variances of the displacements of the collimated and focused beams can be theoretically calculated using [8]:

$$\langle \rho_c^2 \rangle_{collimation} = 0.97 C_n^2 (2a_0)^{-1/3} z^3 \tag{2.27}$$

$$\langle \rho_c^2 \rangle_{focus} = 1.10 C_n^2 (2a_0)^{-1/3} z^3 \tag{2.28}$$

where, a_0 represents the outlet diameter of the transmitting end.

Figure 2.6 demonstrates the relationships of the ratio of the drift of the uniaxial beams to that of the collimated beams with the distance z and focal length F. As discovered in the figure, the beam drifts of the three kinds of light beams are arranged in an ascending order, namely, divergent beam < collimated beam < convergent beam. Particularly, when the focused beams are focused on 35% of the transmission path, the beam drift reaches the maximum value. Since the approximation in geometrical optics is valid merely in the weak fluctuation regions where the intensity variance is $\sigma_I^2 < 1$, the results of formulas (2.27) and (2.28) coincide well with the measured beam drift. While for the strong fluctuation region

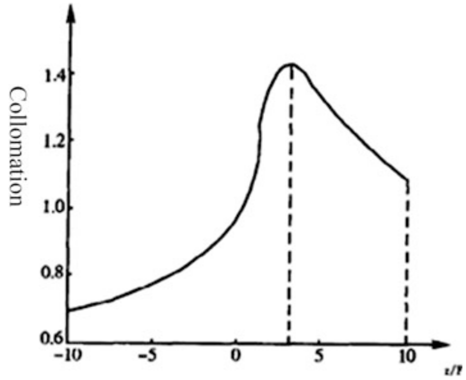

Fig. 2.6 The relationship between the beam drift and the ratio *Z*/*F* of the distance to the focal length

with the intensity variance being $\sigma_I^2 > 1$, it calls for a new theoretical model. The research results demonstrate that the beam drift is expected to present the saturation effect: it is not supposed to increase with the increase of the distance z and C_n^2, under certain a condition, and the range of the beam drift can reach 8 cm.

2.3 Target Modulation of Lasers

The target modulation of lasers is the basis for conducting the target detection based on the laser imaging. The analysis of the mechanism and model of the target modulation of the laser signals is expected to provide a theoretical support for the recognition of the target detection.

2.3.1 The Characteristics and Analytical Method of the Target Modulation of Lasers

1. The characteristics of the target modulation of lasers

   (i) Various action modes: the interaction between the targets and the incident laser gives rise to the phenomena such as reflection, scattering, absorption and transmission, and thus changes the energy and direction of the laser. What's more, the characteristics such as the material, shape, hierarchy and fluctuation of the targets are expected to change the intensity, width and shape of the waveform of the laser echoes. In this way, the characteristics of the waveform of the laser echoes are changed, so as to endow the laser echoes with the aforementioned characteristics of the targets.

   (ii) Complicated modulation mechanism: the parameters such as intensity, width and shape of the pulse of the laser echoes are influenced by the characteristics including the material, shape, hierarchy and fluctuation of the targets.

Meanwhile, modulation factors are mutually coupled, and the strict relationship and accurate influence mechanism for the modulation factors to modulate the laser signals are complicated.

(iii) The difficulty in precise description: in order to understand the characteristics of the targets, it requires to establish the mathematical model of the mapping relation between the echo parameters and the target characteristics based on the characteristics such as the waveform of the laser echoes. However, it is difficult to establish the mathematical model due to the complicated mechanisms and various action models of the modulation of the laser signals using the targets with different characteristics. Thereby, precisely describing the modulation relationship between the characteristics of the targets and the laser signals cannot be easily realized.

2. Methods for analyzing the characteristics of the target modulation of lasers

The theoretical analysis, laboratory measurement of the target materials and scaled models, and static and dynamic measurement of the full-scale target sites can be adopted to study the characteristics of the target modulation of lasers [3].

Theoretical analysis is primarily utilized to reveal the interaction mechanism between the targets and the incident lasers. As an important approach to study the reflection and scattering characteristics of the targets for the lasers, theoretical analysis plays an equal role with the other two methods. Without being mathematically modeled, the data measured in the experiment cannot be favorably utilized to design the lidar, laser imaging and the target detection system based on laser imaging.

The static and dynamic measurement of the full-scale target sites is a basic approach used for quantitatively analyzing the reflection and scattering characteristics of the lasers. As to the principle, it firstly measures relevant data, which are then verified using the mathematical model. By doing so, the accurate data used for describing the parameters are obtained and then employed to design and evaluate the system proposed.

The laboratory measurement of the target materials and scaled models is another important method to study the reflection and scattering characteristics of the targets for the lasers. Compared with the static and dynamic measurement of the full-scale target sites, laboratory measurement is endowed with the following characteristics including simple equipments, readily controlled environmental conditions, convenient repeated measurement and low measurement cost. Laboratory measurement is divided into two types, namely, the measurement of the bidirectional reflectance distribution function (BRDF) of the materials and the measurement of the scaled models. The BRDF of the surface materials of the targets is an important factor determining the characteristics of the target modulation of lasers. According to the BRDF of the surface materials and the geometric parameters of the targets, the laser radar cross section (LRCS) of the targets can be estimated. Therefore, the BRDF measurement of the materials is of great importance for the theoretical analysis and modeling. The measurement of the scaled models is important for it can reveal the characteristics of the modulation of the lasers using the targets with different structures. Meanwhile, it can obtain the numerical relationship between the modulation results and the structure of the targets. However, it presents great measuring difficulty. This is because it is difficult to establish the scaled model and analyze the scale factors in the optical frequency regions. Meanwhile, it is not easy to obtain the characteristics of the modulation of lasers by actual targets through processing and reversing the data measured using the scaled models.

2.3.2 The Modulation Characteristics of the Laser Echoes Energy

According to the detection range equation of lasers, the power of the laser echo is not only related to the atmosphere and the reception performance of the optical system, but also the characteristics of the target itself. These characteristics mainly include the reflection and scattering abilities of the targets for lasers, which are relevant to the type of the surface materials, surface roughness and geometric structure of the targets. Therefore, the reflection and scattering abilities of the targets for lasers are actually the reflection and scattering abilities of the target surface for the lasers. The parameters that can specifically characterize the reflection and scattering properties of the targets for lasers include the reflectivity, BRDF and LRCS.

1. **BRDF**

The reflection on the surface of the targets is divided into the specular and diffuse reflections according to different surface roughnesses. However, as a matter of fact, there exists no absolute specular and diffuse reflections, and the two kinds of reflections are generally interwoven at different degrees. As a result, the distribution curve of the reflection obtained through actual measurement is distorted, and cannot be simply regarded as the specular reflection or diffuse reflection. It is also inappropriate to linearly superpose the components of the two kinds of reflections. Therefore, a parameter that can describe different reflection conditions is required here, so as to accurately reflect the reflection performance of the targets for lasers. Hence, BRDF is adopted as one of the characteristic parameters to describe the reflection performance of the surface of the targets.

According to the geometric distribution shown in Fig. 2.7, it is assumed that the light source with the radiance being L is radiated and uniformly illuminates the isotropous surface A_i. Then, the luminous flux on the bin dA_i nearby the point (x_i, y_i) of the light being emitted from the solid diagonal entry $d\omega_S$ along the direction $s(\theta_S, \varphi_S)$ is expressed as:

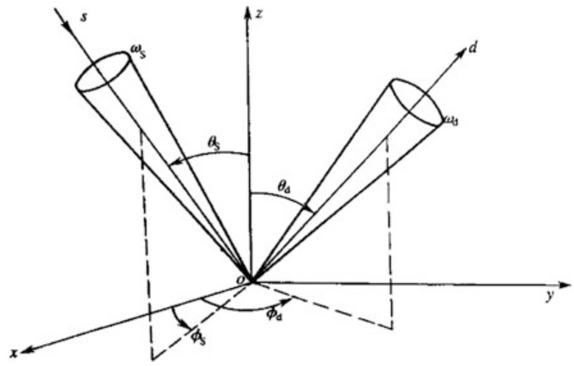

Fig. 2.7 The geometrical relationship of BRDF

$$d^2\Phi_i = L_i \cos\theta_S d\omega_S dA_i = dE_i dA_i \tag{2.29}$$

where, dE_i indicates the irradiance of the light source on dA_i, and L_i represents the radiance on dA_i.

$$dE_i = L_i \cos\theta_S d\omega_S \tag{2.30}$$

As a general rule, the radiance L_r of the reflected light is in direct proportion to the luminous flux on the plane A_i, namely:

$$d^2 L_r = Sd^2\Phi = SdE_i dA_i \tag{2.31}$$

where, the proportional coefficient S is related to the irradiation position, and the incident and detection direction d of the incident light:

$$S = S(\theta_S, \varphi_S, x_i, y_i; \theta_d, \varphi_d) \tag{2.32}$$

The contribution of the whole plane A_i to the radiance of the reflected light can be obtained through solving the integral of formula (2.32):

$$f_r(\theta_S, \varphi_S; \theta_d, \varphi_d) = \int\limits_{A_i} S(\theta_S, \varphi_S, x_i, y_i; \theta_d, \varphi_d) dA_i \tag{2.33}$$

It is defined that:

$$dL_r = dE_i \int\limits_{A_i} S(\theta_S, \varphi_S, x_i, y_i; \theta_d, \varphi_d) dA_i \tag{2.34}$$

According to formula (2.34), we obtain:

$$f_r(\theta_S, \varphi_S; \theta_d, \varphi_d) = \frac{dL_r(\theta_S, \varphi_S; \theta_d, \varphi_d; E_i)}{dE_i(\theta_S, \varphi_S)} \tag{2.35}$$

where, $f_r(\theta_S, \phi_S; \theta_d, \phi_d)$ is called the BRDF of the targets, and is the ratio of the radiance of the reflected light in the direction (θ_d, φ_d) to the irradiance dE_i of the incident light in the solid diagonal entry $d\omega_S$ in the direction (θ_S, φ_S). The value range is from 0 to infinity, with the unit being sr^{-1}. As a differential component, f_r cannot be measured directly, but its average value can be acquired by being measured within the scope of non-zero parameters.

2. **Reflectivity**

Reflectivity $\rho(\omega_S, \omega_d, L_i)$ is an important characteristic parameter describing the reflection characteristics of the surface of the targets for the lasers, and is defined as the ratio of the reflected radiation flux to the incident radiation flux. The incident radiation flux on the bin dA_i within the solid angle ω_S is demonstrated as follows:

$$d\Phi_i = dA_i \int\limits_{\omega_S} L_i(\theta_S, \phi_S) \cos\theta_S d\omega_S \tag{2.36}$$

The reflected radiation flux $d\Phi_r$ measured within the solid angle ω_S is expressed as:

$$d\Phi_r = dA_i \iint\limits_{\omega_S \omega_d} f_r(\theta_S, \phi_S; \theta_d, \phi_d) L_i(\theta_S, \phi_S) \cos\theta_S \cos\theta_d d\omega_S d\omega_d \tag{2.37}$$

Thus, the reflectivity $\rho(\omega_S, \omega_d, L_i)$ is formulated as:

$$\rho(\omega_S, \omega_d, L_i) = \frac{dA_i \iint_{\omega_S \omega_d} f_r(\theta_S, \phi_S; \theta_d, \phi_d) L_i(\theta_S, \phi_S) \cos\theta_S \cos\theta_d d\omega_S d\omega_d}{\int_{\omega_S} L_i(\theta_S, \phi_S) \cos\theta_S d\omega_S} \tag{2.38}$$

If the incident radiation within the incident light beams is isotropous and uniform, then the L_i in formula (2.38) is a constant. Thereby, we obtain:

$$\rho(\omega_S, \omega_d) = \frac{\iint_{\omega_S \omega_d} f_r(\theta_S, \phi_S; \theta_d, \phi_d) \cos\theta_S \cos\theta_d d\omega_S d\omega_d}{\int_{\omega_S} \cos\theta_S d\omega_S} \tag{2.39}$$

Since ω_S and ω_d individually contain three conditions, namely, orientation ($\omega = 0$), cone ($\omega < 2\pi$) and hemisphere ($\omega = 2\pi$), there exit 9 different reflectivities. Formula (2.39) represents the reflectivity of the double-cones. f_r can be considered as a constant within ω_S if the value of ω_S is very small. Then, the reflectivity $\rho(\theta_S, \phi_S; \omega_d)$ of the directional-cone can be obtained, namely:

$$\rho(\theta_S, \phi_S; \omega_d) = \int\limits_{\omega_d} f_r(\theta_S, \phi_S; \theta_d, \phi_d) \cos\theta_d d\omega_d \tag{2.40}$$

Similarly, the reflectivity $\rho(\theta_S, \varphi_S; 2\pi)$ of the directional-hemisphere can be obtained:

$$\rho(\theta_S, \phi_S; 2\pi) = \int\limits_{\omega_d} f_r(\theta_S, \phi_S; \theta_d, \phi_d) \cos\theta_d d\omega_d \tag{2.41}$$

In this way, other reflectivities under different geometric conditions of the incidence and detection can be obtained. The 9 reflectivities describe the 9 possible combinations of the geometric conditions of the incident and reflected beams. Therefore, when referring to the reflectivity, the geometric condition of the incident and reflected beams has to be provided.

Although there exists no absolute diffuse and specular reflections, many conditions are approximated as the diffuse reflection or specular reflection in practice for the sake of simplicity.

The surface with complete diffuse reflection is also called the Lambertian surface, the reflected radiance of which is isotropous within the hemispheric solid angles, that is, the value of the reflected radiance is same in all the direction (θ_d, φ_d). According to the definition of BRDF, we obtain:

$$\begin{aligned} L_r(\theta_d, \phi_d) &= \int f_r(\theta_S, \phi_S; \theta_d, \phi_d) dE_i \\ &= \int f_r(\theta_S, \phi_S; \theta_d, \phi_d) L_i(\theta_S, \phi_S) \cos\theta_S d\omega_S \end{aligned} \tag{2.42}$$

Therefore, it can be seen that in order to make the reflected radiance unrelated to (θ_S, φ_S), f_r has to be a constant. Thus, for a Lambertian surface, formula (2.42) can be simplified as:

$$f_{r,d} = \frac{L_{r,d}}{E_i} \tag{2.43}$$

where, the subscript d indicates there exists a relationship with the Lambertian surface.

The cone-hemisphere reflectivity of the Lambertian surface can be obtained according to the definition of reflectivity:

$$\rho(\omega_S, 2\pi) = \frac{\iint_{\varpi_S \varpi_d} \cos\theta_S \cos\theta_d d\omega_S d\omega_d}{\int\limits_{\varpi_S} \cos\theta_S d\omega_S} = f_{r,d} \cdot \pi \tag{2.44}$$

Thereby, the BRDF of the Lambertian surface is formulated as:

$$f_{r,d} = \frac{\rho(\omega_S, 2\pi)}{\pi} \tag{2.45}$$

Under the condition of complete specular reflection, reflected beams comply with the law of reflection, namely, $\theta_d = \theta_S, \varphi_d = \varphi_S \pm \pi$. Meanwhile, the reflected radiance $L_r(\theta_d, \varphi_d)$ is directly proportional to the incident radiance $L_i(\theta_d, \varphi_{d\pm\pi})$, that is:

$$L_r(\theta_d, \varphi_d) = \rho_{sp} L_i(\theta_d, \varphi_{d\pm\pi}) \tag{2.46}$$

where, ρ_{sp} represents the specular reflectivity.

The f_r of the complete specular reflectivity is an impulse function δ:

$$f_{r,sp}(\theta_S, \varphi_S; \theta_d, \varphi_d) = 2\rho_{sp}(\sin^2\theta_d - \sin^2\theta_S)\delta(\varphi_d - \varphi_{d\pm\pi}) \tag{2.47}$$

3. **LRCS**

LRCS is a physical quantity describing the scattering ability of the targets to the radiated laser. It is defined that when the light intensity generated on the receiver is equal to that generated by a sphere with total reflection, the cross sectional area of the sphere is the LRCS of the targets.

The LRCS of the sphere target is expressed as:

$$\sigma_d = \rho_d \pi r^2 \tag{2.48}$$

where, ρ_d and r indicate the reflectivity and radius of the sphere respectively.

Generally speaking, the more approximate the target to a sphere, the closer the relationship between the LRCS and the size of the target is, while the less the correlation with the orientation and azimuth.

The commonly used methods to establish the calculation model of the laser scattering on the targets include the Kirchkoff's approximation (physical optics method), geometrical optics method, perturbation method, dual-structure method and so on. However, due to the random surface structure of the targets, the aforementioned methods present drawbacks including great workload and time consumption while being used for calculating the distribution of the lasers scattered by the targets. From the perspectives of the feasibility and practicability of the projects, measuring the BRDF of the surface materials is simpler. Then, the effective cross section of the targets for reflecting lasers is calculated according to the test on the geometric structure of the given target.

(1) Estimation of the LRCS

As to the full-scale target characterized by the backscattering with a fixed incident angle, its surface can be divided into many small bins dA_i. Then, the LRCS

$\sigma(\xi, \eta)$ of the whole target can be obtained by performing the area integral on the backscattering coefficient $f_r(\theta_d)$:

$$\sigma(\xi, \eta) = \int_{A_i} \pi f_r(\theta_d) \cos^2 \theta_d dA_i \tag{2.49}$$

where, ξ and η represent the angle parameters between the direction of the incident light and the proprio-coordinate of the target. θ_d indicates the angle between the incident light and the normal line of the target surface, while A_i represents the surface area of the projection of the lasers on the target.

Thus, the relationship between the BRDF and the LRCS is established. The LRCS of the targets can be obtained as long as the analytical expressions of the BRDF and geometric shape of the targets are known.

There are simpler methods to obtain the LRCS of the targets with simple geometric shapes. The backscattering cross section of the targets is generally determined by the product of the reflectivity and irradiated sectional area of the targets. Then, this characteristic quantity can be favorably described by measuring the width of the reflected beams on the targets. The microwave scattering based method can be employed to define LRCS:

$$\sigma = \rho_0 G A_0 \tag{2.50}$$

where, ρ_0 represents the reflectivity of the target surface, while A_0 and G indicate the actual projection area and the optical gain of the targets respectively.

$$G = \frac{4\pi A_c}{\lambda^2} = \frac{4\pi}{\Omega_r} \tag{2.51}$$

where, Ω_r and A_c denote the backscattering solid angle and the coherence area separately, and:

$$A_c = \frac{\lambda^2}{\Omega_r} \tag{2.52}$$

It can be seen from formula (2.50) that ρ_0, A_0 and G are all variables. ρ_0 has been discussed above, and A_0 is the function of the direction of the target type. G is determined by the materials, surface condition, and direction of the targets.

According to Lambertian's law, the cross section areas of several targets with simple geometric shapes are deduced as follows:

(1) For spheres

$$A_0 = \frac{8}{3} a \pi r^2 \tag{2.53}$$

(2) As to planes and plates

$$A_0 = 4a\pi \cos^2 \beta_x \tag{2.54}$$

(3) As for cylinders

$$A_0 = 2a\pi rl \cos^2 \beta_x \tag{2.55}$$

(4) Regarding hemispheres

$$A_0 = \frac{8}{3}a\pi r^2 (1 + \frac{\sin 2\beta_x + 2\beta_x}{2\pi}) \tag{2.56}$$

(5) For cones

$$A_0 = \frac{2a\pi r^2}{\sin \varphi}(\sin \beta_x \cos^2 \varphi + 2\cos^2 \beta_x \sin \varphi) \quad 0 < \beta_x < \varphi, \varphi \le \pi \tag{2.57}$$

where, a and r represent the coefficient and radius respectively. l and ϕ indicate the length of the cylinder and the half-angle of the cone respectively, while β_x denotes the incident angle of lasers.

By calculating the cross section areas of these targets with different shapes, the LRCSs of high resolution of these targets and the complex-shaped targets constituted by these shapes can further be obtained.

(2) The LRCS of typical targets

The laser scattering ability of the targets is related to the surface toughness and geometric structure of the targets. Therefore, different surface toughnesses and geometric structures of the targets lead to the different LRCSs which characterize the laser scattering ability of the targets. The LRCSs of some typical targets are demonstrated as follows.

(i) Targets with specular reflection: a perfect reflecting sphere is defined as a kind of the targets with specular reflection. Specular echoes can be generated on any spherical objects when the root mean square of the surface toughness is far smaller than the wavelength of the lasers.

① Solid corner reflector: since the projection area of the reflector reduces with the increase of the incident angle, the LRCS of the corner reflector is approximately in direct proportion to the cosine of the incident angle (for small angles).

The LRCS of the solid corner reflector is demonstrated as:

$$\sigma = 4\pi \frac{l^4}{3\lambda^2} \tag{2.58}$$

where, l represents the side length of the solid corner reflector, and λ indicates the wavelength of the incident lasers.

When the curvature of the laser signals reflected by the corner reflector is smaller than $\lambda/4$, formula (2.58) is still valid.

② Reflecting plates: the LRCS of the reflecting plates is related to the coatings and the shape of the plates, and the cross sectional area is 100–1500 times greater than that of the original plates with white coatings and diffuse reflection.

(ii) Targets with diffuse reflection: diffuse reflection takes place when the root mean square of the surface toughness of the targets is equal to or slightly greater than the wavelength of the lasers. The amplitude and distribution of the reflected light can be represented by BRDF. The BRDF of the targets with diffuse reflection is determined by many special factors related to the material of the targets. The BRDF of the targets with special materials requires to be determined according to the experimental measurement.

(iii) Targets with Lambertain surfaces: Targets with Lambertain surfaces refer to the targets on which the intensity of the scattered light complying with the Lambert cosine law. As pointed in the law, the light intensity (the flux of the solid angles per unit) reflected from any a direction on the surface of the materials is in direct proportion to the cosine of the angel between this direction and the normal line on the surface.

The LRCS σ of the Lambertain plate with the cross section smaller than that of the transmitted beams is expressed as:

$$\sigma = 4\pi\rho r^2 \cos\theta \tag{2.59}$$

where, ρ and r represent the hemisphere reflectivity on the Lambertain surface and the radius of the Lambertain plate respectively, while θ signifies the incident angle (rad) of the laser source on the Lambertain surface.

The ideal Lambertain reflection surface is able to completely depolarizing the incident lights. However, as a matter of fact, there exist few ideal Lambertain surfaces, and the ideal Lambertain surface is assumed while analyzing problems. Therefore, the polarized LRCS of actual Lambertain targets is 1/2 of the non-polarized LRCS.

(iv) Point targets: formulas (2.58) and (2.59) can be applied in the point targets which are far smaller than beam diameters while beam distribution function is stochastic.

(v) Extended targets: the target detection system based on laser imaging is endowed with narrow beamwidth, and the widths of some targets (ground vehicles or airplanes) are always greater than the beamwidth. Under such circumstance, the LRCS of the Lambertain surface is demonstrated as:

$$\sigma = \pi \rho \varphi^2 r^2 \tag{2.60}$$

where, the definitions of each parameter are same to those of the aforementioned ones.

(vi) Linear targets: the diameter of the linear targets is usually greater than the light beams in certain a direction, and electric wires are the special example of the linear targets. The LRCS of the electric wires or thin targets with diffuse reflection is exhibited as:

$$\sigma = 4 \rho D_w \varphi r \tag{2.61}$$

where, D_w represents the diameter of the cross section of the electric wires (m), and the definitions of other parameters are demonstrated above.

What is worth noting is that formulas (2.60) and (2.61) are established based on the precondition that the surface of the targets is uniformly irradiated, and these formulas need to be used in combination with the distribution functions of the homogeneous beams. Similarly, electric wires and cables contain components of the specular reflection that have strong intensity and are related to the wavelength of the irradiated lasers as well. At present, it has been discovered that the angular position and chord of the components of the specular reflection are associated with the torsional angle of naked electric wires or the wiring harnesses in cables.

(vii) Targets with high resolution: as for the target detection system based on laser imaging, the phenomenon that targets are outside of the resolution cells of the system is likely to occur due to the narrow width of light beams. Under such circumstance, merely part of the targets scatters the laser beams in the resolution cells. In addition, when the short pulses utilized in the detection system cannot illuminate the whole subject simultaneously, but illuminate the target segmentally, the receiver can only receive the light intensity reflected by part of the targets. Under these conditions, the LRCS cannot be represented by a single value. Different irradiation positions on the targets lead to different LRCS.

2.3.3 *The Modulation Characteristics of the Waveform of the Laser Echoes*

After the pulse signals of lasers undergo the space and reflectivity modulation of the targets, the signals received by the detector presents a time-domain modulation waveform. The information contained in this waveform mainly includes the characteristics of the space fluctuation and reflectivity, as well as the distribution law of the targets.

The laser pulses emitted from the laser present Gaussian lineshape in time domain, and the power of the transmitted lasers is demonstrated as [9]:

$$P(t') = P_0 \exp[-\frac{k(t' - \tau/2)^2}{\tau^2}] \tag{2.62}$$

where, P_0 represents the maximum power in the center of the light beams, and $k = 4\ln 2$. τ denotes the half-power width of the laser pulses, while t' indicates the time delay relative to the starting point of the transmitted pulses.

Formula (2.62) represents the waveform that is in symmetrical relationship with $t' = \tau/2$, and the starting point of the transmitted pulses is $t' = 0$.

As for the basic-mode lasers, the spatial distribution of the light intensity also shows Gaussian lineshape, namely:

$$I(r) = I_0 \exp(-\frac{r^2}{w^2}) \tag{2.63}$$

where, represents the central intensity of the laser beams. As demonstrated in Fig. 2.8, $w = w_0\sqrt{1 + \left(\lambda z/\pi w_0^2\right)^2}$, and w denotes the radius of the laser beam at the place presenting the distance of z to the beam waist. Thereinto, w_0 and λ represent the radius of the beam waist and the wavelength of the lasers respectively, while r signifies the distance between a certain point in the laser beam presenting a distance of z to the beam waist and the center of the beams. Laser beams are emitted

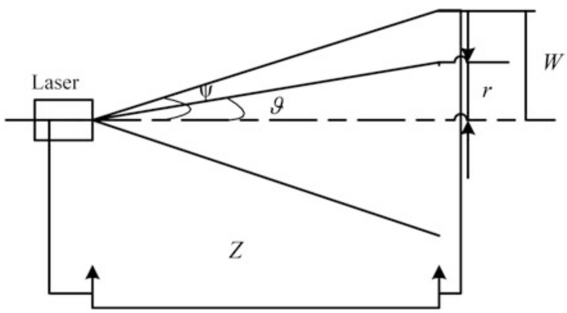

Fig. 2.8 Parameters related to the pulsed laser beams

in the form of wave beams at a divergence angle, and if α represents the half divergence angle of the laser beams, we obtain:

$$\alpha = \lim_{z\to\infty} \frac{dw}{dz} = \frac{\lambda}{\pi w_0} \tag{2.64}$$

As shown in Fig. 2.8, it is assumed that the angel between a line (connected by a point with the radius being r and the laser) and the central axis of the beams is $\psi(-\alpha \le \psi \le \alpha)$. Then, formula (2.63) can be converted into the following formula by using the expressions of α and w when the condition $\lambda z / \pi w_0^2 \ge 1$ in the case of far fields is satisfied.

$$I(\psi) = I_0 \exp(-\frac{2tg^2\psi}{\alpha^2}) \tag{2.65}$$

Thereby, the temporal and spatial distribution of the power of the transmitted laser beams can be expressed as [9]:

$$P(t', \psi) = P_0 \exp[-\frac{k(t' - \tau/2)^2}{\tau^2}] \cdot \exp(-\frac{2tg^2\psi}{\alpha^2}) \tag{2.66}$$

where, P_0 signifies the maximum power in the center of the light beams.

As demonstrated in Fig. 2.9, as the emitted laser beams present a divergence angle, when the target is illuminated by the laser beams, all parts of the target contribute to the laser echoes. Under such circumstance, it is considered that the echoes reflected from the target are caused by the joint imaging of the various points on the target for the laser echoes. The echoes reflected from each point are mutually superposed on the receiving photosensitive surface to form the compound echo. However, the adoption of the direct laser detection gives rise to the loss of the

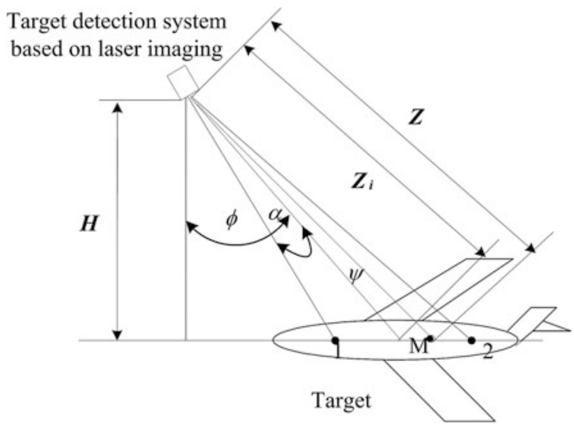

Fig. 2.9 The irradiation of the laser beam on the target

phase information of each sub-echo, and therefore, the compound echo is represented by the superposition of the powers of each echo. As exhibited in Fig. 2.9, α indicates the half divergence angel of lasers, and ψ represents the angel between the line passing through any a point and the central axis of the laser beam. ϕ signifies the angle between the central axis of the laser beam and the nadir of the system.

As demonstrated in Fig. 2.9, H denotes the vertical distance from the laser and detector to the target, and the area between the points 1 and 2 represents the irradiation range of a beam on the target. M is an arbitrary point between 1 and 2. All the points between 1 and 2 are expected to emit the backscattering laser signals with the duration equal to the pulse width. For the convenience of analysis and maintaining the generality, it is assumed that the target being analyzed is in one dimension. The purpose is to find out the time relation of the waveform of the echo pulses. It is obtained that there is always a point M with the distance to the laser being z in the irradiation area at any a moment t within the waveform of the pulses to make $z = ct/2$ valid. Apart from the contribution of the backscattering power of the point M, many points located between the points 1 and 2 contribute to the received power at the moment t. However, according to the assumption of the time domain of the transmitted pulses shown in formula (2.63), as for the transmitted pulses with the width being τ, merely the echoes scattered by the points with the distance z_i to the detector satisfying the condition of $z_i = z - ct'/2$ $(0 \le t' \le \tau)$ can reach the detector simultaneously at the moment t. Therefore, it is concluded that merely the points to the left of the point M have contributions to the echo power at the moment t.

According to the principle of the backscattering of the laser detection, the power received by the detector is the product of the transmit power and a propagation factor $\gamma(z)$. The power at the moment t can be obtained through spatial integral, namely:

$$P_R(t) = \int_{\psi_2}^{\psi_1} P_T(\psi, t')\gamma(z_i)d\psi \tag{2.67}$$

Thereinto:

$$\gamma(z_i) = S_r \rho A(z_i)/z_i^2 \tag{2.68}$$

where, $\gamma(z_i)$ represents the propagation factor with the receiving field angle greater than the divergence angle of lasers of the large targets, and S_r indicates the effective receiving area. ρ denotes the reflectivity of the targets, and is generally considered to be consistent in various directions. $A(z_i)$ is the double-pass total attenuation system of lasers related to the distance, and is assumed as a constant A for the convenience of analysis.

It can be seen from Fig. 2.9 that:

$$z_i = H/\cos(\phi + \psi)\,(-\alpha \le \psi \le \alpha) \tag{2.69}$$

$$t' = t - 2H/c \cdot \cos(\phi + \psi) \tag{2.70}$$

By introducing formulas (2.66), (2.68), (2.69) and (2.70) into formula (2.67), we obtain:

$$P_R(t) = \frac{P_T S_r \sigma A}{\pi} \int_{\psi_2}^{\psi_1} \exp\left[-\frac{k}{\tau^2} \cdot \left(t - \frac{2H}{c \cdot \cos(\phi + \psi)} - \frac{\tau}{2}\right)^2 - \frac{2tg^2\psi}{\alpha^2}\right] \cdot \frac{\cos^2(\phi + \psi)}{H^2} d\psi \tag{2.71}$$

It can be seen from formula (2.71) that the power distribution of the pulses of the laser echoes in time domain is related to the directional angle ϕ and divergence angle α of the wavebeam, the vertical distance H to the target, and the width τ of the transmitted pulses. However, in practical laser scanning detection, the values of α, H and τ are basically constants, merely the value of ϕ keeps changing.

2.4 Typical Target and Atmospheric Modulations

2.4.1 Typical Target Modulation

The target modulation of lasers directly determines the characteristics of the pulse of the laser echoes, specifically, changing the energy and waveform of the echo pulses. In the following part, the modulation of the typical factors including the shape, fluctuation and reflectivity of the targets to the pulse of laser echoes are analyzed.

1. **The modulation using the target with a tilted surface**

When the laser detection is performed on the targets with a tilted surface, a common condition is taken into account, that is, beams irradiate the inclined surface at certain an angle. This is a commonly seen working mode of laser imaging at present. In this part, the relationship between the waveform of the echoes and the inclined surface is discussed.

When lasers illuminate the target obliquely, the relationship between the laser beams and the target is demonstrated in Fig. 2.10. Assume that the laser source transmits laser beams to the target obliquely at the point A, and laser beams are received in the emitting axis. Meanwhile, it is considered that the targets within the laser spots are flat, and the half divergence angle of the laser beams is α.

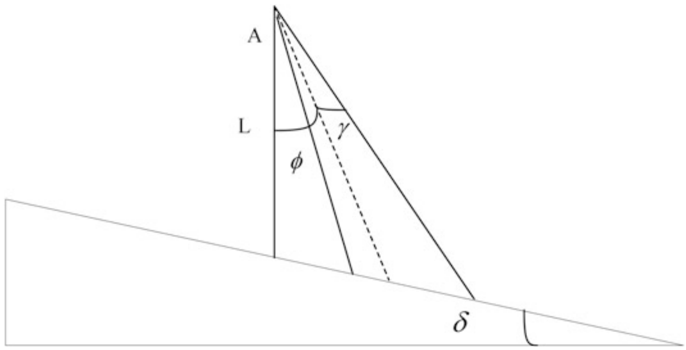

Fig. 2.10 The situation when laser beams irradiate the target obliquely

The height difference within the light spots leads to the enlarged time delay of the echoes on each point, and thus increases the width of the echo pulses. The broadening of the echoes in one dimension is formulated as:

$$\tau = \frac{4L\,\sin(\delta+\phi)\cos(\delta+\phi)\sin\gamma}{c\,\cos(\delta+\phi+\gamma)\cos(\delta+\phi-\gamma)} \tag{2.72}$$

where, L represents the vertical distance from the detector to the inclined plane, and δ denotes the dip angle of the ground. ϕ and γ signify the angle between the central axis and the nadir, and the half width of the light beams respectively.

Figure 2.11 illustrates the relationship between the dip angle and the broadening of the echoes in case L and γ are 300 m and 3 mrad respectively, and ϕ is 0°, 10° and 20°.

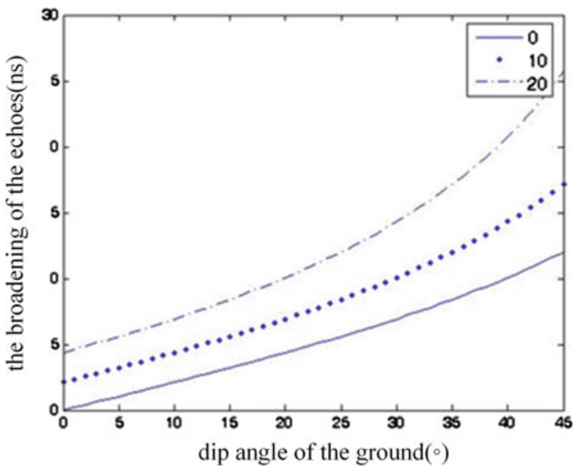

Fig. 2.11 The relationship between the dip angle of the ground and the broadening of the echoes

As discovered in Fig. 2.11, with the increases of the surface slop and dip angle of the irradiation of the laser beams, the broadening of the waveform of the pulses is gradually increased. Then, the increased broadening of the pulses is expected to decrease the receiving power of the echoes, and thus reduce the SNR of the echoes. This finally leads to the increased ranging error and reduced ranging precision. However, the relationship between the broadening of the echo pulses and the slope of the targets and the variation of the frequency components of the echoes caused by the increased broadening of the echo pulses can be obtained. This provides important basis for the extraction of target features in laser detection and the inversion of the attributes of the targets.

2. **The modulation using the targets with a fluctuant surface**

As for the targets with a fluctuant surface, the surface can be divided into the uniformly distributed rough surface and the surface with strong fluctuation. The uniformly distributed rough surfaces such as grasslands and ordinary rocks are endowed with small height variation on the surface. The density function of the height distribution on the surface is generally utilized to describe the roughness. For ordinary targets, it is assumed that they comply with the Gaussian distribution:

$$P_b(H) = \frac{1}{\sqrt{2\pi\sigma_b^2}} \exp\left(-\frac{H^2}{2\sigma_b^2}\right) \tag{2.73}$$

where, σ_b represents the root mean square of the height distribution.

Figure 2.12 illustrates the condition when laser beams illuminate the target with a rough surface. Laser echoes can be regarded as the reconvolution of the transmitted pulses,the response of the planar targets and the roughness function. Therefore, when the height of the target surface shows small fluctuations, it mainly

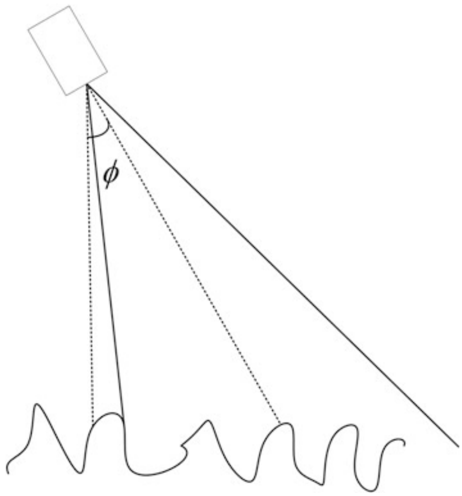

Fig. 2.12 The illumination of a rough surface by the lasers

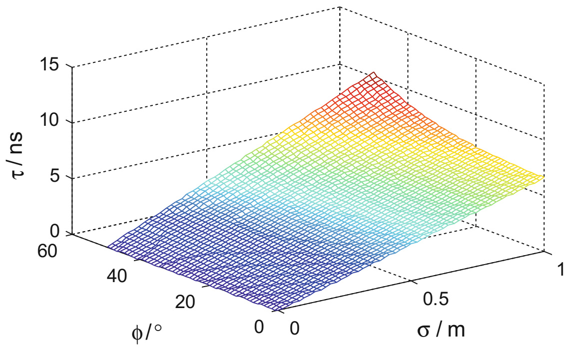

Fig. 2.13 The relationships of the broadening of the echoes with σ_b and ϕ

results in the broadening effect of the echo pulses while having a little influence on the waveform of the echoes.

If the root mean square of the height distribution of the surface is σ_b, the broadening of the echoes caused by the surface fluctuation can be expressed as:

$$\tau = \frac{2\sigma_b}{c\cos\phi} \tag{2.74}$$

where, ϕ indicates the angle between the radiated lasers and the nadir. The broadening, and the variations of the echoes of laser pulses radiated by the nanosecond lasers with the root mean square σ_b with height distribution and the angel ϕ are demonstrated in Fig. 2.13.

When the target surface presents strong fluctuations within the light spots, the violent height variation of the target surface is expected to result in the increased difference in time delay of the echoes reflected from different points. This kind of surface includes trees and buildings on the ground, airplanes in the air, and ships at sea. As a result, the broadening of the compounded echoes is supposed to increase as well. Besides, when the time delay difference caused by the different time-delays of the echoes from each point is increased to some extent, the waveform of the echoes is expected to be changed and even fractured to form multiple sub-echoes. Figure 2.14 illustrates the echo waveform of the small trees in the lawn being obliquely illuminated in the experiment. Under such circumstance, the small trees are regarded as the strong fluctuation in the lawn.

As discovered in Fig. 2.14, a laser echo is broken into two sub-echoes. Thereinto, the first and second sub-echoes represent the echoes from the small trees and the lawn respectively. Meanwhile, the first sub-echo is fractured to form three peaks. The reason for the generation of this waveform is the great height difference between the small trees and the lawn. As a result, part of the laser beams is reflected by the crown or the lawn directly, while some illuminate the lawn after penetrating through the gaps in the crown and then reflected back by the lawn. Finally, two echoes are compounded in the time domain while reaching the detector. As the crown is endowed with certain thickness, and the branches and leaves in the crown

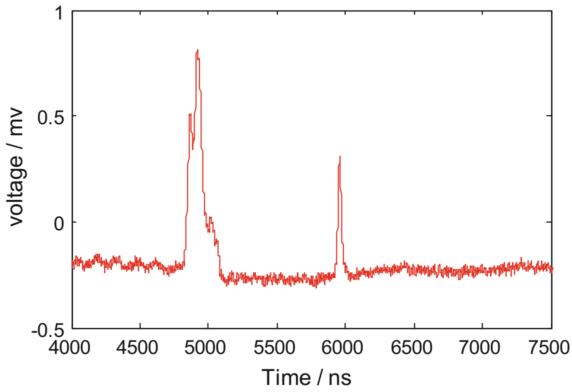

Fig. 2.14 The echo waveform of the small trees in the lawn

present complicated height distribution, broadening and fracturing occur to the first echo.

3. **The modulation based on the variation of surface reflectivity of the targets**

According to the analysis above, the echo signals of lasers are the superposition of the echoes reflected from each point in the target within the light spots. When the reflectiveity of the surface in the laser spots changes, the waveform characteristics of the echoes are expected to change accordingly. As for the actual targets, the surface reflectivity varies in most situations. For example, in earth observations, different surface reflectivities can be found in the junctions of the vegetations, water surfaces and snowfields with the bare lands, and the boundaries between the cement ground and the vegetations. The phenomenon can also be discovered for the targets in the air and at sea with different surfaces, as well as the boundaries between the paints and other materials. Due to the different surface reflectivities, the energy of the laser echoes reflected from each point does not coincide with Gaussian distribution any more in airspace. The waveform of the compounded echoes is therefore changed. Figure 2.15 illustrates the one-dimensional simulation results of the echoes reflected from the terrains with same height distribution but different distributions of the reflectivity.

Given the target detection system based on laser imaging uses the pulse laser, the broadening of the laser echoes reflected from the targets has a great influence on the imaging of the targets. Firstly, in reduces the vertical resolution of the target detection based on a laser imaging system. The vertical resolution is inversely proportional to the width of the laser pulses: the narrower the laser pulses, the higher the resolution. Therefore, the existence of the broadening increases the pulse width to some extent, and thus virtually reduces the range resolution. Secondly, it affects the ranging precision. The ranging precision is closely related to the measurement precision of the time delay of the echoes. However, the broadening of the laser echoes reflected by the targets damages symmetry and uniformity of the front and back edges of the echo pulses present, causing the rising and falling edges

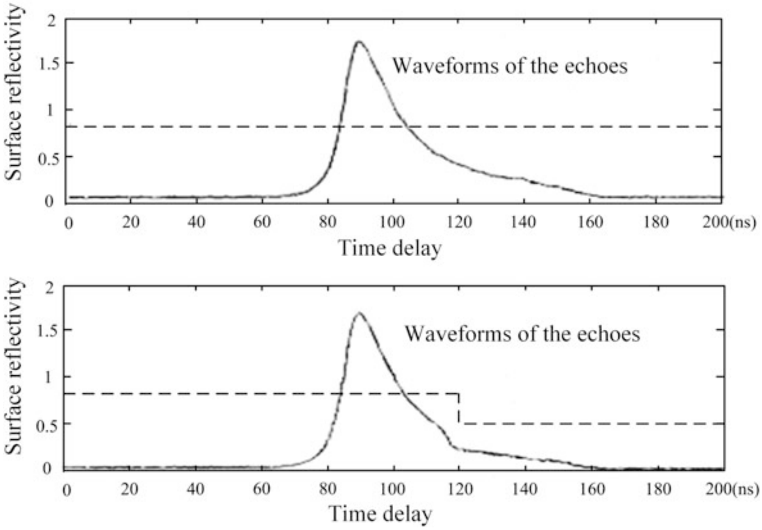

Fig. 2.15 Comparison of the waveforms of the echoes reflected from the terrains with different distributions of the reflectivity

losing the symmetric relation. As a result, the time distribution of the energy of the echoes fluctuates, which reduces the measurement precision of the time based on the energy. Furthermore, it affects the ranging precision and then the precision of the range profile. In addition, the broadening of the echo waveforms is expected to reduce the echo power and thus affect the operating range of the imaging detection. Additionally, the broadening of the laser echoes is supposed to change the waveform of the laser echoes. For the waveform based imaging detection mode for identifying the attributes of the targets, there exists a mapping relation between the waveform of the laser echoes and the targets. However, while performing the target identification using the matching method, the irregular variation of the waveform of the echoes is expected to give inaccurate detection results.

2.4.2 Typical Atmospheric Modulation

Due to the modulation of the typical factors including the atmospheric absorption, scattering and turbulence of the lasers, the phenomena such as wavefront distortion, intensity scintillation and beam extension generally take place on the laser echoes. As a result, these phenomena give rise to the reduced SNR and resolution of the imaging system, which thus affects the receiving, processing, image quality and detection results of the target detection system based on laser imaging.

1. Atmospheric absorption and scattering reduce the SNR of the imaging system, the operating range, and the image quality

Both the atmospheric absorption and scattering can reduce the flux of the given light beams [8]. Atmospheric scattering does not change the internal energy of the molecules, while atmospheric absorption gives rise to the variation of the energy state.

As a laser with a determined wavelength propagates in the atmosphere, according to the Lambert-Bougner law, we obtain:

$$P_{\lambda}(x) = P_{\lambda_0} \exp(-\mu(\lambda)x) \tag{2.75}$$

where, P_{λ_0} represents the laser power at $z = 0$, and $P_{\lambda}(x)$ indicates the power of the lasers after propagating in the atmosphere for a distance of x.

Thereby, the attenuation degree of the lasers after propagating in the atmosphere for the distance of x is obtained:

$$\begin{aligned} \tau(\lambda) &= \frac{P_{\lambda}(x)}{P_{\lambda_0}} = \exp(-\mu(\lambda)x) \\ &= \exp(-\alpha(\lambda)x) \cdot \exp(-\gamma(\lambda)x) \\ &= \tau_{\alpha}(\lambda) \cdot \tau_{\gamma}(\lambda) \end{aligned} \tag{2.76}$$

It can be seen that the atmospheric absorption and scattering make the echo power of the lasers received by the system become $\tau_{\alpha}(\lambda) \cdot \tau_{\gamma}(\lambda)$ when the lasers propagate in free spaces. In case the noise is constant, the SNR of the imaging system is expected to become the normal $\tau_{\alpha}(\lambda) \cdot \tau_{\gamma}(\lambda)$.

For the target detection system based on laser imaging, the ranging precision is inversely proportional to the square root of the SNR of the echo signals. Therefore, the higher the SNR, the higher the ranging precision is. The greater the distance precision is, the more accurate the distance profile of the targets obtained in the range imaging; and vice versa. The declined SNR caused by the atmospheric absorption and scattering inevitably reduces of the ranging precision and thus the image quality.

2. Atmospheric turbulence changes the broadening of the pulse width and the echo waveform, and thus affects the precision of the detection

One of the influences of the atmospheric turbulence is the beam extension. The existence of the bean extension leads to the subtle variation of the dips of the radiated light beams on the various sampling points of the targets. Meanwhile, the paths between the various points in the light spots and the optical receiving system are expected to be changed as well, which gives rise to the variation of the time delay of the echoes reflected from the various sampling points on the targets. Afterwards, the superposition of the laser echoes reflected from different points broadens the pulse width of the laser echoes, and thus damages the symmetry between the front and back edges of the pulses.

3. Atmospheric turbulence reduces the azimuth resolution and the image resolution

One of the advantages of the target detection system based on laser imaging is the narrow beam width, which contributes to the high azimuth resolution. However, one of the influences of the atmospheric turbulence on the laser propagation is to diverge the lasers. In this way, the width of the laser beams is increased. Since the azimuth resolution is generally 1/2 of the beam width, the azimuth resolution is therefore reduced.

There exists the following relationship between the pixel of the laser images and the field of view:

$$P = \frac{FOV}{M} \tag{2.77}$$

where, P is the size of the pixel, and determines the image resolution. FOV and M represent the field angle and the image matrix of the lasers on the targets respectively. Atmospheric turbulence is expected to diverge the lasers, which actually increases the field angle and spot area of the lasers. The increase of the spot area leads to the increased blur degree of the sampled targets, and thus reduces the size of the image matrix. According to formula (2.77), the increased field angle and reduced matrix inevitably lead to the reduction in the image resolution.

References

1. Krawczyr R, Goretta O, Kassighian A (1993) Temporal pulse extension of a return lidar signal. Appl Opt 32(33):6784–6788
2. Zhao N, Hu Y (2006) Relation of laser remote imaging signal and object detail identities. Infrared Laser Eng 35(2):226–229
3. Dai Y (2010) LiDAR (volume 1). Publishing House of Electronics Industry, Beijing
4. Chen X (2006) Atmospheric environment and microwave laser weapons. Chinese People's Liberation Army Publishing House, Bejing
5. McCartney EJ (1988) Atmospheric optical molecules and particle scattering (trans: Pan N, Mao J et al.). Science Press, Beijing
6. Song Z (1990) Elements of applied atmospheric optics. China Meteorological Press, Bejing
7. Xiong F (1994) LIDAR. Astronavigation Press, Beijing
8. Zhang Y, Chi Q (eds) (1997) The propagation and imaging of the light waves in the atmosphere. National Defense Industry Press, Bejing
9. Hu Y, Wei Q, Liu J et al (1997) An analysis of the characteristics of the return pulse in airborne laser beam scanning. Appl Laser 17(3):109–111

Springer

http://www.springer.com/978-981-10-3496-1

Theory and Technology of Laser Imaging Based Target Detection
Hu, Y.
2018, XIII, 333 p. 185 illus., 68 illus. in color., Hardcover
ISBN: 978-981-10-3496-1